Since January 2020 Elsevier has created a COVID-19 resource centre with free information in English and Mandarin on the novel coronavirus COVID-19. The COVID-19 resource centre is hosted on Elsevier Connect, the company's public news and information website.

Available online at www.sciencedirect.com
SCIENCE DIRECT®
Biochemical and Biophysical Research Communications 334 (2005) 79–85
BBRC
www.elsevier.com/locate/ybbrc

Susceptibility of human and rat neural cell lines to infection by SARS-coronavirus

Makiko Yamashita, Masanobu Yamate, Gui-Mei Li, Kazuyoshi Ikuta *

Department of Virology, Research Institute for Microbial Diseases, Osaka University, Suita, Osaka 565-0871, Japan

Received 25 May 2005
Available online 22 June 2005

Abstract

Pathological characterization of autopsied tissues from patients with SARS revealed severe damage in restricted tissues, such as lung, with no apparent cell damage in other tissues, such as intestine and brain. Here, we examined the susceptibility of neural cell lines of human (OL) and rat (C6) origins to SARS-associated coronavirus. Both of the neural cell lines showed no apparent cytopathic effects (CPE) by infection but produced virus with infectivity of 10^{2-5} per ml, in sharp contrast to the production by infected Vero E6 cells of $>10^9$ per ml that showed a lytic infection with characteristic rounding CPE. Interestingly, the infection of intestinal cell line CaCo-2 also induced no apparent CPE, with production of the virus at a slightly lower level as that of the Vero E6 cell culture. Notably, the cellular receptor for the virus, angiotensin-converting enzyme 2 was expressed at similar levels on Vero E6 and CaCo-2 cells, but at undetectable levels on OL and C6 cells.

Keywords: SARS; Coronavirus; Neural cells; Vero E6; CaCo-2; OL; C6; ACE2

The coronaviruses (CoVs) are enveloped, positive-strand RNA viruses. Severe acute respiratory syndrome (SARS)-CoV was identified as an etiological agent of an acute infectious respiratory disorder [1–4]. Infection by this virus shows features typical of acute infectious disease within a short incubation period.

Pathological characterization of autopsied tissues from SARS-CoV-infected individuals revealed viral signals in the lung and small intestine [5,6]. The lung and small intestine were confirmed to be positive for angiotensin-converting enzyme 2 (ACE2) [7], which was identified as the host cell receptor for infection of this virus [8]. In addition, SARS-CoV was also shown to be positive by in situ hybridization and immunohistochemistry in organs and tissues other than the lung and intestine, i.e., kidney, liver, and cerebrum, but not in spleen and cerebellum, from all four of the SARS autopsies examined [5]. Thus, SARS-CoV signal was positive in cerebrum, although ACE2 expression was positive only in endothelial and smooth muscle cells in the brain sections [7].

Generally, CoVs are well known to infect and establish persistent infections in neural cells in vitro as well as in vivo, as has been demonstrated for mouse hepatitis virus (MHV) [9–16] and human CoVs OC43 [17] and 229E [18]. Recently, the mode of SARS-CoV infection was reported using C57BL/6 mice [19]. In that report, it was shown that a clinical isolate of SARS-CoV could replicate transiently to high levels in the ACE2-positive lung of intranasally infected mice. Surprisingly, infection spread to the brain after it was cleared from the lung. Consequently, the authors concluded that C57BL/6 mice undergo transient nonfatal systemic infection with this virus in the lung, which is able to disseminate to the brain. In this study, we examined the susceptibility of neural cell lines derived from human and rat origins, OL and C6, respectively, to SARS-CoV. The results showed that both cell lines, which

* Corresponding author. Fax: +81 6 6879 8310.
E-mail address: ikuta@biken.osaka-u.ac.jp (K. Ikuta).

0006-291X/$ - see front matter © 2005 Elsevier Inc. All rights reserved.
doi:10.1016/j.bbrc.2005.06.061

express undetectable levels of ACE2, supported the replication of this virus, although the replication levels were extremely low compared with those of other susceptible cell lines, such as Vero E6 and CaCo-2.

Materials and methods

Virus. The Vero E6 cell line was used for propagation of SARS-CoV (Frankfurt-1 strain) [20]. Vero E6 cells were maintained in MEM (Gibco BRL) supplemented with 10% fetal bovine serum (FBS; ICN Flow), 100 U/ml penicillin, and 100 μg/ml streptomycin (Gibco BRL) (complete medium), and passaged every 3 days. The inoculum of SARS-CoV was the culture medium from infected Vero E6 cells collected at 3 days post-infection and filtered through a cell strainer to remove cell debris, and then stored at −80 °C. The virus titers were determined in 96-well microplates with Vero E6 cells as 50% tissue culture infectious dose $(TCID)_{50}$/ml using Karber's method [21].

Infection with SARS-CoV. In addition to Vero E6, the following cell lines were examined for infection by SARS-CoV: human oligodendroglioma-derived cell line OL [22] which was generated at the Wistar Institute, Philadelphia, USA [23]; rat glioma-derived cell line C6 [24]; human intestine-derived cell line CaCo-2; canine kidney-derived cell line MDCK; rabbit kidney-derived cell line RK13. All these cells were similarly infected with SARS-CoV at a multiplicity of infection (MOI) of 10. After adsorption for 1 h, the cells were cultured in MEM supplemented with 2% FBS.

Reverse transcription-polymerase chain reaction. For reverse transcription (RT)-polymerase chain reaction (PCR) to detect SARS-CoV genome RNA, total RNA was extracted from infected cells with TRIzol (Invitrogen). The RNA was reverse-transcribed with SuperScript III Reverse Transcriptase (Invitrogen) using the primer 5′-TCTTGATGGATCTGGGTAAGGC-3′ (complementary to nucleotides 15,857–15,878 in open reading frame 1ab). The cDNA was amplified from the viral genomic RNA with ExTaq (Takara, Kyoto, Japan) using primers 5′-GAATCCTGACATCTTACGCG-3′ (nucleotides 13,871–13,890) and 5′-TGTTAGGCATGGCTCTGTCA-3′ (nucleotides 15,255–15,236). For the detection of mRNA for SARS-CoV S protein, cDNAs prepared as described above with oligo(dT) primer (Invitrogen) were amplified using primers 5′-GGAAAAGCC AACCAACCTCGATCTC-3′ (nucleotides 23–47, corresponding to the common leader sequence) and 5′-ACTACATCTATAGGTTGA TAGCCCT-3′ (nucleotides 22,084–22,108). For detection of the mRNA for N protein, the same cDNAs were amplified using the same leader primer and the primer 5′-AGGAAGTTGTAGCACGGTGGC AGC-3′ (nucleotides 28,585–28,608). The primers were prepared according to the genome sequence of SARS-CoV reported previously [25]. For RT-PCR to detect mRNA of ACE2, total RNA was extracted from uninfected cells with TRIzol. The cDNAs prepared with oligo(dT) primer from Vero E6, CaCo-2, and OL cells of human and monkey origins were amplified using forward primer (5′-ATGTC AAGCTCTTCCTGGCTCCTTC-3′) and reverse primer (5′-CTA AAAGGAGGTCTGAACATCATCAG-3′) for human ACE2 (Accession No. NM_021804). The cDNAs prepared from C6 of rat origin with oligo(dT) primer were amplified using forward primer (5′-ATGTCAAGCTCCTGCTGGCTCCTTC-3′) and reverse primer (5′-TTAGAATGAAGTTTGAGCATCATCAC-3′) for rat ACE2 (Accession No. NM_001012006). As a control for the input RNA, levels of a housekeeping gene, glyceraldehyde-3-phosphate dehydrogenase gene (GAPDH) were also assayed using forward primer 5′-ACC ACAGTCCATGCCATCAC-3′ and reverse primer 5′-TCCAC-CACC CTGTTGCTGTA-3′. The intensity of each band was quantified with NIH image software.

Antibodies specific to SARS-CoV. Murine monoclonal antibody (MAb) 3A2 recognizing SARS-CoV S protein was obtained by immunizing mice with SARS-CoV particles that were purified by centrifugation of the conditioned media of infected Vero E6 cells collected at 3 days post-infection through 20% (w/v) sucrose in phosphate-buffered saline (PBS). In addition, the following anti-SARS-CoV polyclonal antibodies (PAbs) were purchased: rabbit PAb to the N-terminus region of SARS-CoV S protein (Cat. No. AP6009b; ABGENT, San Diego, USA) and rabbit PAb to the C-terminus region of SARS-CoV N protein (Cat. No. AP6005b; ABGENT).

Immunofluorescence (IF). The infected cells were trypsinized, and the resulting single cells were smeared and then fixed with cold acetone. The fixed cells were reacted with murine MAb 3A2, then with the second antibody, fluorescent isothiocyanate (FITC)-conjugated goat anti-mouse IgG (Jackson ImmunoResearch Laboratories, West Grove, USA).

Membrane IF and flow cytometry for ACE2. For membrane IF and flow cytometry, the unfixed cells were reacted with anti-ACE2 PAb (anti-human ACE2 ectodomain antibody; Research and Diagnostic Systems) followed by second antibody, then subjected to IF microscope (Nikon ECLIPSE E-600) and flow cytometry (FACSCalibur; Becton–Dickinson).

Western blotting. Uninfected or infected cells were solubilized in SDS–polyacrylamide gel electrophoresis (PAGE) sample buffer and the resulting samples were subjected to 10% SDS–PAGE, and then Western blotted onto polyvinylidene difluoride membranes (Millipore, Bedford, USA). After blocking with 5% skim milk in PBS containing 0.05% Tween 20 (PBST), the membranes were incubated with rabbit anti-SARS-CoV S and N PAbs. As a control, the membrane was incubated with murine MAb to α-tubulin (Sigma; clone B-5-1-2). After washing with PBST, the membranes were reacted with a horseradish peroxidase (HRP)-conjugated second antibody, goat anti-rabbit IgG, and donkey anti-mouse IgG (Jackson ImmunoResearch Laboratories), respectively.

Results

Neural cell lines, OL of human origin and C6 of rat origin, were similarly infected with SARS-CoV at an MOI of 10. After adsorption for 1 h, the cells were washed with PBS and cultured. As controls, Vero E6, CaCo-2, MDCK, and RK13 cells were similarly infected with SARS-CoV. The cell proliferation rates of the infected cells in triplicate experiments revealed that only the Vero E6 cell number declined even in the next day after infection, while all the other cells showed proliferation that were almost similar as those of uninfected parental cells (Fig. 1A). In fact, severe cytopathic effects (CPE) appeared only in infected Vero E6 cells on day 2 post-infection, while all of the other cell lines, including CaCo-2 and neural cell lines, representatively showed no apparent CPE (Fig. 1B). To detect the SARS-CoV infection in the neural cell lines, the viral antigen expression in the cells was examined by an IF test on day 2 post-infection (Fig. 1C). Strong IF-staining with anti-SARS-CoV S MAb (3A2) was detected in the cytoplasmic region of infected Vero E6 and CaCo-2 cells. In both infected OL and C6 cells, the number of cells with clear IF-staining was much lower (Fig. 1C). There were no apparent IF-positive cells in MDCK and RK13 cells (Fig. 1C). The culture media from the same Vero E6 and CaCo-2 cells 1 and 2 days post-infection, used in

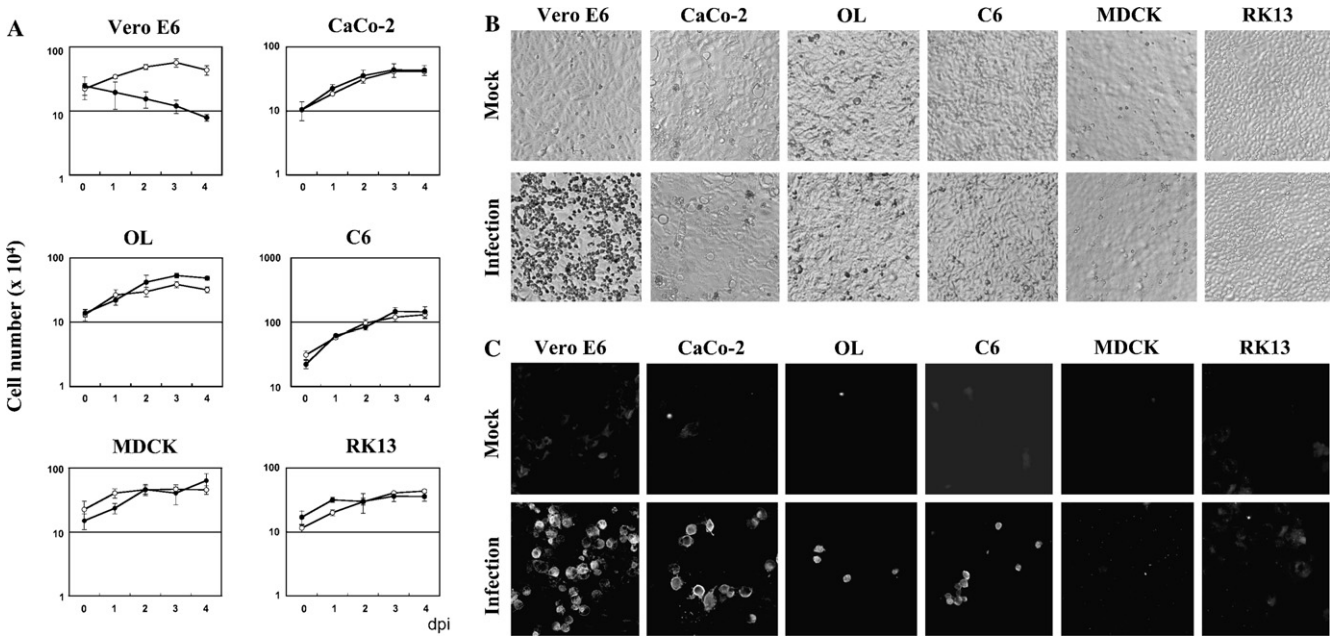

Fig. 1. No apparent CPE on neural cell lines during the acute phase of SARS-CoV infection. Monolayers of a total of six cell lines, Vero E6, CaCo-2, OL, C6, MDCK, and RK13 in 24-well microplates were similarly mock-infected and infected with SARS-CoV at an MOI of 10. After adsorption for 1 h at 37 °C, the cells were washed three times with PBS, and then cultured with MEM supplemented with 2% FBS, with replacing with fresh medium on day 2 post-infection. (A) The viable adherent cell numbers of mock-infected (○) and infected (●) cells at each day post-infection were estimated by trypan blue dye exclusion. The data are shown by means of triplicate experiments. (B) The morphology of individual mock-infected and infected cells on day 2 post-infection was observed by phase contrast microscope to look for the appearance of CPE. (C) The same cell cultures as in Fig. 1B on day 2 post-infection were subjected to an IF test with anti-SARS-CoV S MAb (3A2).

Fig. 1A, were subjected to the infectivity titration. The results showed that the titer was highest in Vero E6 and slightly lower in CaCo-2, that were very contrast to those in OL and C6 neural cells (Fig. 2). The titers in the culture media on day 2 post-infection were slightly increased compared to those on day 1 post-infection in all these infected cells. In contrast, the infectivity titers were almost negligible in the culture media from infected

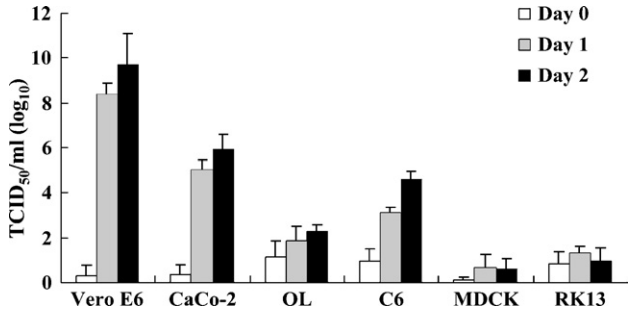

Fig. 2. Only a low titer of virus infectivity of SARS-CoV was detected in the culture media from infected neural cell lines. The culture media from the same cell cultures in Fig. 1 on days 0 (no incubation in medium after adsorption followed by washing with PBS), 1, and 2 post-infection were subjected to infectivity titration using Vero E6 cells as described under Materials and methods. The $TCID_{50}$/ml obtained in individual infected cells are shown by means of triplicate experiments.

MDCK and RK13 cells and there were no apparent differences between the titers on days 1 and 2 post-infection.

To confirm the expression of SARS-CoV in the neural cell lines, we next examined the presence of viral RNA by RT-PCR. First, amplification of the viral genomic RNA by RT-PCR with a primer set located in open reading frame 1ab was examined (Fig. 3A). A clear discrete band was detectable by RT-PCR of the RNA extracted from OL and C6 cells, as well as MDCK and RK13 cells, 2 days post-infection, and the mobility of the band corresponded to that of the band detected by RT-PCR with the RNA from Vero E6 and CaCo-2 cells 2 days post-infection. Again, the amounts of the above RT-PCR products were slightly higher in infected Vero E6 and CaCo-2 cells than infected OL, C6, MDCK, and RK13 cells, all of which showed similar levels. Next, we used primers from the S (Fig. 3B) and N (Fig. 3C) regions to amplify viral mRNA species. Using S primers, a clear band was detectable only for Vero E6 and CaCo-2 cells and only a faint band was detected in OL cells, but the other infected cells showed no detectable band. In contrast, by using N primers, a clear difference was found in the patterns of RT-PCR products among individual infected cells. Several mRNA species encompassing the region overlapping the N region could be identified at high levels in Vero

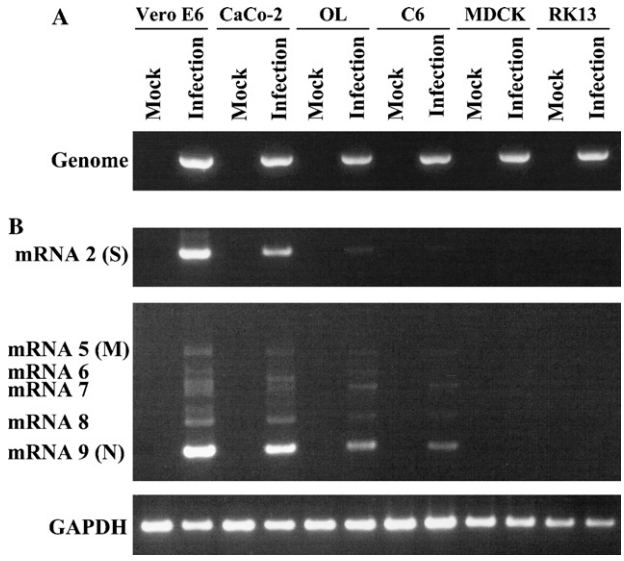

Fig. 3. SARS-CoV replication in infected neural cells at low levels. Total RNAs were extracted from the Vero E6, CaCo-2, OL, C6, MDCK, and RK13 cells mock-infected and infected with SARS-CoV on day 2 post-infection, similarly prepared as described in Fig. 1. (A) The RNAs were used for quantification of the SARS-CoV genome by semi-quantitative RT-PCR. (B) The same RNAs were used for amplification of SARS-CoV S and N mRNAs. As a control, housekeeping gene GAPDH was amplified using the same RNA preparations.

E6 and CaCo-2 cells. In addition, similar mRNA species were also detected in OL and C6 cells, but at lower levels. In contrast, there were no bands corresponding to such mRNA species in MDCK or RK13 cells. These results may indicate that SARS-CoV expression and replication occur in OL and C6 cells at significantly lower levels compared with those in Vero E6 and CaCo-2 cells, while there was no apparent evidence to support the expression and replication of this virus in MDCK and RK13 cells. The positive PCR signals in MDCK and RK13 cells for viral genomic RNA (Fig. 3A) might have derived from the adsorbed SARS-CoV particles. Consequently, OL and C6 cells were found to be susceptible to SARS-CoV, although the viral expression levels were greatly lower compared with those in infected Vero E6 and CaCo-2 cells.

Western blotting of the infected OL and C6 cells also supported the notion of a much lower level of viral expression in infected OL and C6 cells compared with infected Vero E6 and CaCo-2 cells (Fig. 4A). Both bands for the N and S proteins of SARS-CoV were clearly identified in Vero E6 cells, while a clear band of the N and only a faint band of the S were identified in CaCo-2 cells. In contrast, the N, but not the S, protein band was only faintly identified in infected OL and C6 cells. The results were confirmed by independently prepared three sets of infected cell samples (Fig. 4B). In all three experiments, level for α-tubulin in infected Vero E6 was significantly decreased. Therefore, when we estimate the relative expression levels of SARS-CoV S and N proteins compared with that of α-tubulin, we might overestimate the S and N protein levels in Vero E6 cells (Fig. 4B).

Next, OL and C6 cells were characterized regarding the expression of ACE2 by membrane IF and flow cytometry, as well as RT-PCR (Fig. 5). The results showed no apparent expression of ACE2 on the OL and C6 cells using anti-ACE2 PAb, which could detect ACE2 expression on ~40% of Vero E6 and ~50% of CaCo-2 cells (Fig. 5A). Furthermore, RT-PCR analysis for ACE2 mRNA revealed no detectable levels of ACE2 expression in OL or C6 cells, even at the transcriptional level (Fig. 5B).

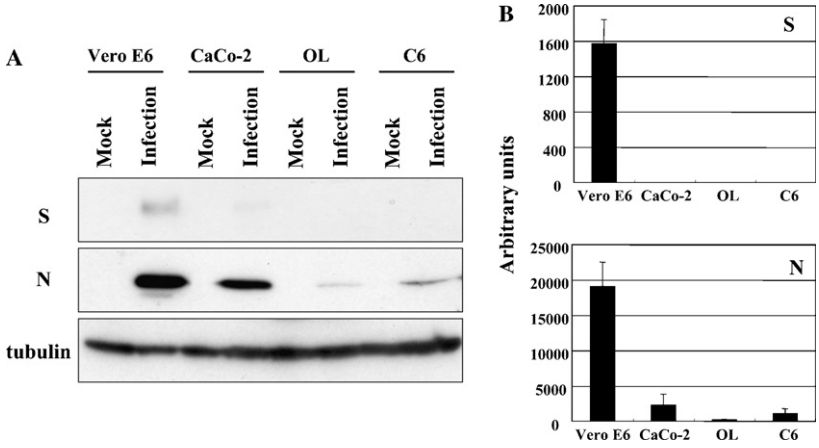

Fig. 4. Viral protein expression in SARS-CoV-infected neural cell lines by Western blot analysis. (A) The Vero E6, CaCo-2, OL, C6 cells mock-infected, and infected with SARS-CoV on day 2 post-infection, similarly prepared as described in Fig. 1, were subjected to Western blotting with PAb to SARS-CoV N and S proteins, and to α-tubulin as a control. Data from one experiment representative of three independent experiments are shown. (B) For quantitative analysis, band intensities were determined with NIH image software. Values were normalized to α-tubulin levels. The data are expressed as means plus standard error.

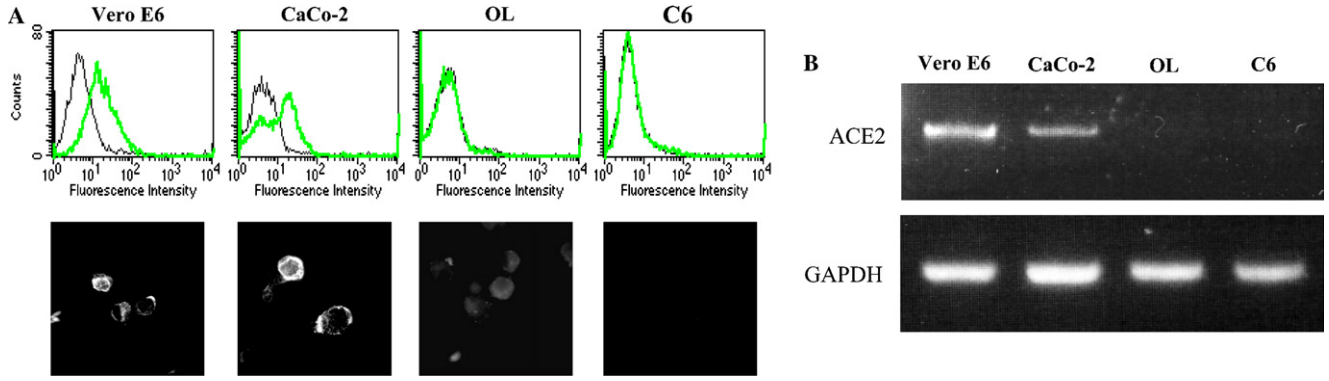

Fig. 5. No expression of ACE2 on neural cell lines derived from humans as well as from rats. (A) The OL and C6 cells were subjected to flow cytometry (upper panels) as well as membrane IF (lower panels) with anti-ACE2 PAb. (B) Total RNA extracted from the same cells used for (A) was subjected to quantitative RT-PCR for ACE2 mRNA using human ACE2 sequence-derived primers for Vero E6, CaCo-2, and OL cells and rat ACE2 sequence-derived primers for C6 cells.

Discussion

Human and rat neural cell lines were shown in this study to be susceptible to infection with SARS-CoV, with no apparent CPE. Both of these cell lines express ACE2 at undetectable levels. The virus particle production rates of both cell lines were markedly lower than those of typical SARS-CoV-susceptible cell lines, such as Vero E6 and CaCo-2. Previously, the susceptibility of 23 [26] and 30 [27] different permanent and primary eukaryotic cell lines to SARS-CoV was studied. However, among the above cells, one murine neural cell line, astrocytoma-derived DBT, was negative for infection to this virus [27].

ACE2 was identified as the host cell receptor for infection with SARS-CoV [8]. In fact, ACE2-positive Vero E6 and CaCo-2 cell lines showed similar high susceptibility to this virus. However, cytopathicity appeared in infected Vero E6 cells, while there was no apparent cytopathicity in infected CaCo-2 cells. Therefore, the expression level of ACE2 seems not to be directly related to the induction of cytopathicity during the acute phase of infection with this virus, although the virus replication rate may be related to the ACE2 expression level.

Pathological characterization of several autopsied tissues from SARS patients revealed viral signals, mostly in ACE2-positive lung and intestine, and in addition, in the brain the SARS-CoV signal was detected in the cerebrum by in situ hybridization and immunohistochemistry at lower levels [5], although the brain was negative for ACE2 expression [7]. Similarly, although lymphoid organs, including peripheral blood mononuclear cells (PBMCs) were also negative for ACE2 [5,6], evidence of long-lasting detectability of SARS-CoV RNA in PBMCs was demonstrated by RT-PCR analysis of infected individuals at different clinical stages [28].

It is noteworthy that OL cells of human origin and C6 cells of rat origin showed similar susceptibility to SARS-CoV infection. This finding leads support to the possibility that the SARS-CoV could be derived from natural virus carriers. In this regard, several reports have shown the susceptibility of various animals to this virus: ferrets and domestic cats [29], various species of monkeys [30,31], civets [32,33], pigs and chickens [34], as well as mice [20,35,36]. Rodents are of particular interest in the study of SARS as a model animal. It was demonstrated that C57BL/6 mice could be productively infected by SARS-CoV in the bronchial and bronchiolar epithelium of the respiratory tract, and that the virus was rapidly cleared through a mechanism independent of lymphoid cells [20]. Compared to human ACE2, murine ACE2 was shown to less efficiently bind the S1 domain of SARS-CoV, and rat ACE2 was even less efficient [37]. However, it is noteworthy that this virus was able to spread to the brain of mice as well as to multiple other organs at late time points when it had already been cleared by the lung [20]. Interestingly, rats in particular have been proposed to be vectors for SARS-CoV, based on circumstantial evidence from Amoy Gardens, Hong Kong [38]. The evidence showing the susceptibility of rat neural cell line C6 to this virus in this study may support this hypothesis.

Acknowledgments

We are grateful to Dr. John Ziebuhr, University of Würzburg, Germany, for giving us the Frankfurt strain of SARS-CoV through Dr. Fumihiro Taguchi, National Institute of Infectious Diseases, Tokyo, Japan. This work was supported in part by a Grant-in-Aid for scientific research from the Ministry of Education, Science, Sports and Culture of Japan and by the 21st Century COE program (Combined Program on Microbiology

and Immunology) from Japan Society for the Promotion of Science.

References

[1] C. Dresten, S. Gunther, W. Preiser, S. van der Werf, H.R. Brodt, S. Becker, H. Rabenau, M. Panning, L. Kolesnikova, R.A. Fouchier, A. Berger, A.M. Burguiere, J. Cinatl, M. Eickmann, N. Esckmann, N. Esckmann, N. Escrion, K. Grywna, S. Kramme, J.C. Manuguerra, S. Muller, V. Rickerts, M. Sturmer, S. Vieth, H.D. Klenk, A.D. Osterhaus, H. Schmitz, H.W. Doerr, Identification of a novel coronavirus in patients with severe acute respiratory syndrome, N. Engl. J. Med. 348 (2003) 1967–1976.

[2] K.V. Holmes, SARS-associated coronavirus, N. Engl. J. Med. 348 (2003) 1948–1951.

[3] T.G. Ksiazek, D. Erdman, C.S. Goldsmith, S.R. Zaki, T. Peret, S. Emery, S. Tong, C. Urbani, J.A. Comer, W. Lim, P.E. Rollin, S.F. Dowell, A.E. Ling, C.D. Humphrey, W.J. Shieh, J. Guarner, C.D. Paddock, P. Rota, B. Fields, J. DeRisi, J.Y. Yang, N. Cox, J.M. Hughes, J.W. LeDuc, W.J. Bellini, L.J. Anderson, A novel coronavirus associated with severe acute respiratory syndrome, N. Engl. J. Med. 348 (2003) 1953–1966.

[4] T. Kuiken, R.A. Fouchier, M. Schutten, G.F. Rimmelzwaan, G. van Amerongen, D. van Riel, J.D. Laman, T. de Jong, G. van Doornum, W. Lim, A.E. Ling, P.K. Chan, J.S. Tam, M.C. Zambon, R. Gopal, C. Drosten, S. van der Werf, N. Escriou, J.C. Manuguerra, K. Stohr, J.S. Peiris, A.D. Osterhaus, Newly discovered coronavirus as the primary cause of severe acute respiratory syndrome, Lancet 362 (2003) 263–270.

[5] Y. Ding, L. He, Q. Zhang, Z. Huang, X. Che, J. Hou, H. Wang, H. Shen, L. Qiu, Z. Li, J. Geng, J. Cai, H. Han, X. Li, W. Kang, D. Weng, P. Liang, S. Jiang, Organ distribution of severe acute respiratory syndrome (SARS) associated coronavirus (SARS-CoV) in SARS patients: implications for pathogenesis and virus transmission pathways, J. Pathol. 203 (2004) 622–630.

[6] K.F. To, A.W.I. Lo, Exploring the pathogenesis of severe acute respiratory syndrome (SARS): the tissue distribution of the coronavirus (SARS-CoV) and its putative receptor, angiotensin-converting enzyme 2 (ACE2), J. Pathol. 203 (2004) 740–743.

[7] I. Hamming, W. Timens, M.L.C. Bulthuis, A.T. Lely, G.J. Navis, H. van Goor, Tissue distribution of ACE2 protein, the functional receptor for SARS coronavirus. A first step in understanding SARS pathogenesis, J. Pathol. 203 (2004) 631–637.

[8] W. Li, M.J. Morre, N. Vasilieva, J. Sui, S.K. Wong, M.A. Berne, M. Somasundaran, J.L. Sullivan, K. Luzuriaga, T.C. Greenough, H. Choe, M. Farzan, Angiotensin-converting enzyme 2 is a functional receptor for the SARS coronavirus, Nature 426 (2003) 450–454.

[9] A. Lucas, M. Coulter, R. Anderson, S. Dales, W. Fintoff, In vivo and in vitro models of demyelinating diseases. II. Persistence and host-regulated thermosensitivity in cells of neural derivation infected with mouse hepatitis and measles viruses, Virology 88 (1978) 325–337.

[10] S.A. Stohlman, A.Y. Sakaguchi, L.P. Weiner, Characterization of the cold-sensitive murine hepatitis virus mutants rescued from latently infected cells by cell fusion, Virology 98 (1979) 448–455.

[11] K.V. Holmes, J.N. Behnke, Biochemistry and biology of coronaviruses, in: V. ter Meulen, S. Siddell, H. Wege (Eds.), Evolution of a Coronavirus during persistent infection in vitro, Plenum Press, New York, 1981, pp. 287–300.

[12] E. Lavi, A. Suzumura, M. Hirayama, M.K. Highkin, D.M. Dambach, D.H. Silberberg, S.R. Weiss, Coronavirus mouse hepatitis virus (MHV)-A59 causes a persistent, productive infection in primary glial cell cultures, Microb. Pathog. 3 (1987) 79–86.

[13] K.V. Holmes, Virology, in: B.N. Fields (Ed.), *Coronaviridae* and their replication, second ed., Raven Press, New York, 1990, pp. 841–856.

[14] J.L. Gombold, S.T. Hingley, S.R. Weiss, Fusion-defective mutants of mouse hepatitis virus A59 contain a mutation in the spike protein cleavage signal, J. Virol. 67 (1993) 4504–4512.

[15] F. Taguchi, T. Ikeda, S. Makino, H. Yoshikura, A murine Coronavirus MHV-S isolate from persistently infected cells has a leader and two consensus sequences between the M and N genes, Virology 198 (1994) 355–359.

[16] S.E. Coley, E. Lavi, S.G. Sawicki, L. Fu, B. Schelle, N. Karl, S.G. Siddell, V. Thiel, Recombinant mouse hepatitis virus strain A59 from cloned, full-length cDNA replicates to high titers in vitro and is fully pathogenic in vivo, J. Virol. 79 (2005) 3097–3106.

[17] N. Arbour, G. Coté, C. Lachance, M. Tardieu, N.R. Cashman, P.J. Talbot, Acute and persistent infection of human neural cell lines by human coronavirus OC43, J. Virol. 73 (1999) 3338–3350.

[18] N. Arbour, S. Ekandé, G. Coté, C. Lachance, F. Chagnon, M. Tardieu, N.R. Cashman, P.J. Talbot, Persistent infection of human oligodendrocytic and neuroglial cell lines by human coronavirus 229E, J. Virol. 73 (1999) 3326–3337.

[19] W.G. Glass, K. Subbarao, B. Murphy, P.M. Murphy, Mechanisms of host defense following severe acute respiratory syndrome-coronavirus (SARS-CoV) pulmonary infection of mice, J. Immunol. 173 (2004) 4030–4039.

[20] K.A. Ivanov, V. Thiel, J.C. Dobbe, Y. van der Meer, E.J. Snijder, J. Ziebuhr, Multiple enzymatic activities associated with severe acute respiratory syndrome coronavirus helicase, J. Virol. 78 (2004) 5619–5632.

[21] J. Karber, Beitrag zur kollectiven Behandlung pharmakologische Reihenversuche, Arch. Exp. Path. Pharmakol. 162 (1931) 480–483.

[22] M. Yamashita, W. Kamitani, H. Yanai, N. Ohtaki, Y. Watanabe, B.J. Lee, S. Tsuji, K. Ikuta, K. Tomonaga, Persistent Borna disease virus infection confers instability of HSP70 mRNA in glial cells during heat stress, J. Virol. 79 (2005) 2033–2041.

[23] Y. Nakamura, H. Takahashi, Y. Shoya, T. Nakaya, M. Watanabe, K. Tomonaga, K. Iwahashi, K. Ameno, N. Momiyama, H. Taniyama, T. Sata, T. Kurata, J.C. de la Torre, K. Ikuta, Isolation of Borna disease virus from human brain tissue, J. Virol. 74 (2005) 4601–4611.

[24] P. Benda, J. Lightbody, G. Sato, L. Levine, W. Sweet, Differentiated rat glial cell strain in tissue culture, Science 161 (1968) 370–371.

[25] V. Thiel, K.A. Ivanov, A. Putics, T. Hertzig, B. Schelle, S. Bayer, B. Weissbrich, E.J. Snijder, H. Rabenau, H.W. Doerr, A.E. Gorbalenya, J. Ziebuhr, Mechanisms and enzymes involved in SARS coronavirus genome expression, J. Gen. Virol. 84 (2003) 2305–2315.

[26] K. Hattermann, M.A. Müller, A. Nitsche, S. Wendt, O.D. Mantke, M. Niedrig, Susceptibility of different eukaryotic cell lines to SARS-coronavirus, Arch. Virol. 150 (2005) 1432–8798.

[27] E.C. Mossel, C. Huang, K. Narayanan, S. Makino, R.B. Tesh, C.J. Peters, Exogenous ACE2 expression allows refractory cell lines to support severe acute respiratory coronavirus replication, J. Virol. 79 (2005) 3846–3850.

[28] H. Wang, Y. Mao, L. Ju, J. Zhang, Z. Liu, X. Zhou, Q. Li, Y. Wang, S. Kim, L. Zhang, Detection and monitoring of SARS coronavirus in the plasma and peripheral blood lymphocytes of patients with severe acute respiratory syndrome, Clin. Chem. 50 (2004) 1237–1240.

[29] B.E. Martina, B.L. Haagmans, T. Kuiken, R.A. Fouchier, G.F. Rimmelzwaan, G. van Amerongen, J.S. Peiris, W. Lim, A.D. Osterhaus, Virology: SARS virus infection of cats and ferrets, Nature 425 (2003) 915.

[30] R.A.M. Fouchier, T. Kuiken, M. Schutten, G. van Amerongen, G.J.J. van Doornum, B.G. van den Hoogen, M. Peiris, W. Lim, K. Stöhr, A.D.M.E. Osterhaus, Koch's postulates fulfilled for SARS virus, Nature 423 (2003) 240.

[31] B.L. Haagmans, T. Kuiken, B.E. Martina, R.A. Fouchier, G.F. Rimmelzwaan, G. van Amerongen, D. van Riel, T. de Jong, S. Itamura, K.H. Chan, M. Tashiro, A.D. Osterhaus, Pegylated interferon-α protects type 1 pneumocytes against SARS coronavirus infection in macaques, Nat. Med. 10 (2004) 290–293.

[32] H.-D. Song, C.-C. Tu, G.-W. Zhang, S.-Y. Wang, L.-C. Lei, Q.-X. Chen, Y.-W. Gao, H.-Q. Zhou, H. Xiang, H.-J. Zheng, S.-W. Wang Chern, F. Cheng, C.-M. Pan, H. Xuan, S.-J. Chen, H.-M. Luo, D.-H. Zhou, Y.-F. Liu, J.-F. He, P.-Z. Qin, L.-H. Li, Y.-Q. Ren, W.-J. Liang, Y.-D. Yu, L. Anderson, M. Wang, R.-H. Xu, X.-W. Wu, H.-Y. Zheng, J.-D. Chen, G. Liang, Y. Gao, M. Liao, L. Fang, L.-Y. Jiang, H. Li, F. Chen, B. Di, L.-J. He, J.-Y. Lin, S. Tong, X. Kong, L. Du, P. Hao, H. Tang, A. Bernini, X.-J. Yu, O. Spiga, Z.-M. Guo, H.-Y. Pan, W.-Z. He, J.-C. Manuguerra, A. Fontanet, A. Danchin, N. Niccolai, Y.-X. Li, C.-I. Wu, G.-P. Zhao, Cross-host evolution of severe acute respiratory syndrome coronavirus in palm civet and human, Proc. Natl. Acad. Sci. USA 102 (2005) 2430–2435.

[33] D. Wu, C. Tu, C. Xin, H. Xuan, Q. Meng, Y. Liu, Y. Yu, Y. Guan, Y. Jiang, X. Yin, G. Crameri, M. Wang, C. Li, S. Liu, M. Liao, L. Feng, H. Xiang, J. Sun, J. Chen, Y. Sun, S. Gu, N. Liu, D. Fu, B.T. Eaton, L.-F. Wang, X. Kong, Civets are equally susceptible to experimental infection by two different severe acute respiratory syndrome coronavirus isolates, J. Virol. 79 (2005) 2620–2626.

[34] H.M. Weingartl, J. Copps, M.A. Drebot, P. Marszal, G. Smith, J. Gren, M. Andova, J. Pasick, P. Kitching, M. Czub, Susceptibility of pigs and chickens to SARS coronavirus, Emerg. Infect. Dis. 10 (2004) 179–184.

[35] K. Subbarao, J. McAuliffe, L. Vogel, G. Fahle, S. Fischer, K. Tatti, M. Packard, W.J. Shieh, S. Zaki, B. Murphy, Prior infection and passive transfer of neutralizing antibody prevent replication of severe acute respiratory syndrome coronavirus in the respiratory tract of mice, J. Virol. 78 (2004) 3572–3577.

[36] T.C. Greenough, G.J. Babcock, A. Roberts, H.J. Hernandez, W.D. Thomas Jr., J.A. Coccla, R.F. Grazlano, M. Srinivasan, I. Lowy, R.W. Finberg, K. Subbarao, L. Vogel, M. Somasundaran, K. Luzuriaga, J.L. Sullivan, D.M. Ambrosino, Development and characterization of a severe acute respiratory syndrome-associated coronavirus-neutralizing human monoclonal antibody that provides effective immunoprophylaxis in mice, J. Infect. Dis. 191 (2005) 507–514.

[37] W. Li, T.C. Greenough, M.J. Moore, N. Vasilieva, M. Somasundaran, J.L. Sullivan, M. Farzan, H. Choe, Efficient replication of severe acute respiratory syndrome coronavirus in mouse cells is limited by murine angiotensin-converting enzyme 2, J. Virol. 78 (2004) 11429–11433.

[38] S.K.C. Ng, Possible role of an animal vector in the SARS outbreak at Amoy Gardens, Lancet 362 (2003) 570–572.